

12 AUG 1948

NATIONAL ADVISORY COMMITTEE FOR AERONAUTICS

TECHNICAL NOTE

No. 1666

FLIGHT INVESTIGATION OF EFFECTS OF ROTOR-BLADE TWIST
ON HELICOPTER PERFORMANCE IN THE HIGH-SPEED AND
VERTICAL-AUTOROTATIVE-DESCENT CONDITIONS

By Alfred Gessow

Langley Aeronautical Laboratory
Langley Field, Va.



Washington
August 1948

NACA LIBRARY
LANGLEY MEMORIAL AERONAUTICAL
LABORATORY
Langley Field, Va.

NATIONAL ADVISORY COMMITTEE FOR AERONAUTICS

TECHNICAL NOTE NO. 1666

FLIGHT INVESTIGATION OF EFFECTS OF ROTOR-BLADE TWIST
ON HELICOPTER PERFORMANCE IN THE HIGH-SPEED AND
VERTICAL-AUTOROTATIVE-DESCENT CONDITIONS

By Alfred Gessow

SUMMARY

Flight-performance measurements were made on an untwisted, plywood-covered rotor in the high-speed and vertical-autorotative-descent conditions. The results were compared with measurements on a similar rotor having 8° of linear washout and with theoretical calculations in order to determine the effects of rotor-blade twist on helicopter performance.

The use of negative blade twist appears to be an effective means for increasing the maximum speed of the helicopter as limited by blade stall and for reducing the performance losses due to stall at a given thrust coefficient and tip-speed ratio. In particular, an increase of approximately 7 miles per hour or about 10 percent in the limiting forward speed of the helicopter seems possible with the use of -8° twist. In terms of profile-drag power savings at a given airspeed, once stalling had developed on both rotors, the rotor profile-drag losses incurred by blade stall could be reduced by approximately 40 percent of the average profile-drag power absorbed by the rotors in the unstalled condition by use of -8° twist.

A comparison of the test results obtained with both rotors in vertical power-off descent showed that negative blade twist had little effect on the performance of the helicopter in that condition. As indicated by limited data, the same conclusion appeared to be true for the forward-flight glide condition as well.

Calculated values obtained from an available semiempirical theory indicated that the measured rates of descent in vertical power-off descent were 6 percent higher than the predicted values. Good agreement was obtained, however, between the theoretical results and the few measured rotor drag-lift ratios obtained in forward-flight autorotative glides.

INTRODUCTION

Rotor-blade twist has often been advocated as an effective means of minimizing the adverse effects of stalling of the retreating blade

of a helicopter rotor traveling at high tip-speed ratios. (See references 1, 2, and 3.) These effects are manifested by increased rotor power losses and by severe vibration and loss of control which ultimately limit the forward speed of the helicopter. An analysis of flight measurements, including measurements obtained in the high-speed condition, on a helicopter rotor having plywood-covered blades that incorporated 8° of linear washout was presented in reference 3. These results afforded the opportunity of verifying experimentally the theoretically-predicted effects of blade twist on high-speed rotor performance if data were available on a similar rotor having untwisted blades. Accordingly, flight measurements were obtained on an untwisted plywood-covered rotor, having the same solidity, plan form, and airfoil sections as the previously tested twisted blades, for the conditions in which blade stalling was present. Because the effects of twist cannot at present be theoretically determined in power-off vertical flight and because of the importance of this condition from considerations of safety and design, the sinking speeds of the helicopter in this condition were also measured in order to determine whether significant differences existed between the untwisted and twisted blades. An analysis of the results of the measurements is presented herein, together with a comparison of the performance of the twisted blades in the same flight conditions.

Some limited data in the forward-flight-climb and autorotative-glide conditions, which were incidentally obtained, are also compared herein with corresponding twisted-blade data. In all cases, the test measurements are analyzed and correlated with calculations obtained by available rotor theory.

SYMBOLS

W	gross weight of helicopter, pounds
b	number of blades per rotor
R	blade radius, feet
r	radial distance to blade element, feet
c	blade-section chord at radius r, feet

c_e	equivalent blade chord, feet	$\left(\frac{\int_0^R cr^2 dr}{\int_0^R r^2 dr} \right)$
-------	------------------------------	---

σ	rotor solidity ($bc_e/\pi R$)
θ	average main rotor-blade pitch at the 0.75 radius, uncorrected for play in linkage or for blade twist caused by air loads, degrees
θ_1	linear blade twist, obtained as difference between root and tip pitch angles, positive when tip angle is greater
ρ	mass density of air, slugs per cubic foot
ρ_0	mass density of air at sea level under standard conditions (0.002378 slugs per cubic foot)
V_c	calibrated airspeed (indicated airspeed corrected for instrument installation errors, considered equal to $V \sqrt{\rho/\rho_0}$ in the present case), miles per hour
V	true airspeed of helicopter along flight path, miles per hour
V_h	horizontal component of true airspeed of helicopter, miles per hour
V_v	vertical component of true airspeed of helicopter, positive in climb, feet per minute
Ω	rotor angular velocity, radians per second
γ	angle of climb $\left(\tan^{-1} \frac{V_v}{88V_h} \right)$
α	rotor angle of attack; angle between projection in plane of symmetry of axis of no feathering and line perpendicular to flight path, positive when axis is pointing rearward, radians (The axis of no feathering is defined as the axis about which there is no first harmonic feathering or cyclic pitch variation.)
μ	tip-speed ratio $\left(\frac{V \cos \alpha}{\Omega R} \right)$

$\Delta\alpha_f$	correction to fuselage angle of attack to allow for rotor downwash, degrees (assumed equal to $\frac{57.3 C_L}{4}$)
α_{fc}	corrected fuselage angle of attack, degrees
α_r	blade-element angle of attack, measured from line of zero lift, radians
$\alpha(1.0)(270^\circ)$	blade-element angle of attack at tip of retreating blade at 270° azimuth angle, degrees
L	rotor lift, pounds
D	rotor drag, pounds
T	rotor thrust, pounds
$C_{L_{uncor}}$	rotor lift coefficient, uncorrected for air loads on fuselage $\left(\frac{W \cos \gamma}{\frac{1}{2} \rho V^2 \pi R^2} \right)$
C_L	rotor lift coefficient $\left(\frac{L}{\frac{1}{2} \rho V^2 \pi R^2} \right)$
C_D	rotor drag coefficient $\left(\frac{D}{\frac{1}{2} \rho V^2 \pi R^2} \right)$
C_T	rotor thrust coefficient $\left(\frac{T}{\pi R^2 \rho (\Omega R)^2} \right)$
$\left(\frac{D}{L} \right)_o$	rotor profile drag-lift ratio
$\left(\frac{D}{L} \right)_{oth}$	rotor profile drag-lift ratio as calculated from theory
$\left(\frac{D}{L} \right)_{exp}$	rotor profile drag-lift ratio as calculated from measured quantities
$\left(\frac{D}{L} \right)_{Pt}$	parasite-drag contribution of tail rotor divided by main-rotor lift

$\left(\frac{D}{L}\right)_{Pf}$	parasite drag of fuselage, rotor head, and blade shanks, divided by main-rotor lift
$\left(\frac{D}{L}\right)_c$	drag-lift ratio representing angle of climb γ , positive in climb
$\left(\frac{D}{L}\right)_i$	rotor induced drag-lift ratio
$\left(\frac{D}{L}\right)_r$	rotor drag-lift ratio; ratio of equivalent drag of rotor to rotor lift $\left(\left(\frac{D}{L}\right)_c + \left(\frac{D}{L}\right)_i\right)$
P/L	shaft power parameter, where P is equal to rotor-shaft power divided by velocity along flight path and is therefore also equal to drag force that could be overcome by the shaft power at flight velocity

APPARATUS AND INSTRUMENTATION

The test rotor was flown on a conventional helicopter, a general view of which is shown in figure 1, and a three-view drawing, including dimensions and pertinent characteristics, is shown in figure 2. A general view of the rotor blade, including its plan-form dimensions, is given in figure 3.

The test rotor differed from the rotor used in the investigation of reference 3 by having zero twist instead of -8° twist. The blade profile and surface condition of the two rotors were quite similar and the airfoil sections of both rotors could be expected to have the same stalling angle. Briefly, the blades were plywood-covered and were designed with an NACA 23015 section having the rearward 10 percent of the mean line reflexed 0.9° . The blade surfaces were refinished before the tests and could be considered aerodynamically smooth, although to build up the forward portion to a true contour as regards shape and maximum thickness was not feasible. The solidity of the rotors was 0.042.

All quantities necessary for the complete determination of the performance of the test rotor were obtained from NACA recording instruments. Particular care was taken in the measurement of airspeed and main-rotor shaft torque because of their critical influence on such final performance parameters as the rotor drag-lift ratio.

Airspeed was determined by means of a freely swiveling pitot-static installation mounted on the end of a long boom in front of the fuselage, the airspeed head being about 2 feet in front of the main rotor disk.

The installation was calibrated by means of a trailing pitot-static "bomb" suspended approximately 100 feet below the rotor. In order to insure zero horizontal airspeed, both recorded and visual indications of longitudinal and lateral velocity deviations from zero airspeed were employed in the vertical descent tests.

The main-rotor-shaft torque was obtained by means of a strain-gage torque-meter, the strain-sensitive elements being mounted on the drive shaft between the gear box and the pylon thrust bearing. The power required by the main rotor was then calculated as the product of the measured torque and rotor rotational speed, the latter being obtained with an NACA recording tachometer.

Photographs of the airspeed installations, as well as a detailed description of the instrumentation and methods employed in the performance measurements, will be found in references 3, 4, and 5.

REDUCTION OF DATA AND THEORETICAL ANALYSIS

Rotor drag-lift ratios were calculated for the forward-flight condition from the general performance equation expressed in coefficient form as

$$\frac{P}{L} = \left(\frac{D}{L}\right)_r + \left(\frac{D}{L}\right)_{p_f} + \left(\frac{D}{L}\right)_{p_t} + \left(\frac{D}{L}\right)_c$$

For each data point, values of P/L , $(D/L)_{p_f}$, $(D/L)_{p_t}$, and $(D/L)_c$ were determined from measured data, as described in reference 4.

Rotor drag coefficients in vertical autorotative descent were obtained from the gross weight of the helicopter, the measured rate of descent, and the air temperature and pressure by the following formula

$$C_D = \frac{W}{\frac{1}{2}\rho V^2 \pi R^2}$$

The flight data are compared with theoretical calculations. Briefly, the performance of the rotor in the level-flight, climb, and glide conditions was computed from the performance charts of reference 6. The semiempirical theory covering the vertical autorotative condition was obtained from reference 7. The profile-drag polar used in the theoretical comparisons is representative of the drag characteristic of well-built plywood-covered blades and is considered to apply to the two sets

of rotor blades tested. Although section data over the working angle-of-attack range are lacking for the untwisted and twisted test rotors, an experimental check on their minimum profile-drag coefficient, obtained by testing the rotor in the zero-thrust region, yielded a value of 0.008, which compared favorably with the value 0.0084 used in the theoretical calculations. Further, the theoretical polar was based on tests of airfoil sections similar to that used in the test rotors. The actual and theoretical polars were therefore assumed to be in agreement.

RESULTS AND DISCUSSION

Level flight.— Test data obtained in forward flight are listed in table I, and the values of main-rotor drag-lift ratios and other parameters derived from these data are given in table II.

Both theoretical considerations and experimental studies have shown that stalling first appears on a helicopter rotor at the tip of the retreating blade. This earlier occurrence of stall at the tip of the retreating blade rather than near the root arises from the fact that the greater rotational speed of the tip sections, combined with the down flow through the rotor disk, results in larger section angles of attack at the tip. For a given operating condition, tip stalling can be reduced by constructing the blade with negative twist, so that the blade tip sections will operate at lower angles of attack on a twisted blade than on an untwisted blade. Although the lower tip angles are obtained at the expense of somewhat higher angles inboard, the highest angles would still occur at the blade tip for the range of twists under discussion (in the neighborhood of 8°).

The degree to which twist would be expected to delay the occurrence of high tip angles is illustrated in figure 4 for the test helicopter at typical operating conditions. The figure shows that, at the same air-speed, the calculated tip angles of attack of the blades having -8° twist are about 2.5° less than those of the untwisted blades over the speed range shown.

The increased stalling to which rotors are subjected at higher forward speeds results in increasing vibration and control difficulties and in higher rotor profile-drag losses. Data showing the effect of rotor-blade stalling, as indexed by the angle of attack of the retreating blade, are shown in figure 5(a) for the untwisted blades and in figure 5(b) for the twisted blades (reference 3). These data are presented in terms of the ratio of measured to theoretical profile-drag-lift ratios plotted as a function of tip angle. The stall data of figures 5(a) and 5(b) are represented by straight-line fairings and for purposes of comparison, the fairing of the data for the twisted blade (fig. 5(b)) is also shown in figure 5(a).

It should be noted that if the tip angle of attack could be precisely calculated for both rotors and if the shape and rate of growth of the stalled areas on both rotors were the same, the faired curves of figure 5(a) should coincide. The difference of approximately $1\frac{1}{4}^\circ$ between the faired data shown on the figure can therefore be attributed to errors in the calculation of the tip angles (which would be primarily due to assumptions regarding the inflow distributions for the blades of different twists) and to differences between the shape and rate of growth of the stalled areas.

The effectiveness of twist in extending the speed range of the helicopter by delaying blade stalling and in reducing the profile-drag power losses due to stall is shown in figure 6, which gives the variation of profile-drag power with speed for the test helicopter at a typical operating condition ($W = 2625$ lb, $\Omega R = 450$ fps, $C_T = 0.0050$). The curves of figure 6 were obtained by combining the variation of speed with tip angle as given by figure 4 with values of profile-drag power computed from the values of the profile drag-lift ratios for the various tip angles given in figure 5. This method of cross-plotting eliminates the need for accurately predicting the difference in tip angles of attack between both rotors by eliminating the tip-angle parameter. The solid-line curves in figure 6 represent the theoretical profile-drag power with no allowance for blade stalling, whereas the dash-line curves represent the theoretical power plus an experimental correction for blade stalling as obtained from figure 5.

The results shown in figure 6 indicate that the theory (with no allowance for stalling) underestimated the rotor profile-drag losses for conditions resulting in calculated tip angles of attack above the stall, the discrepancy increasing rapidly with the speed. The figure also shows that stalling losses began at a speed 7 miles per hour (about 10 percent) higher with the twisted blades than with the untwisted blades. In this connection it might be noted that if the previously discussed $1\frac{1}{4}^\circ$ discrepancy in tip angles in figure 5(a) was applied to the curves of figure 4 as a correction factor, the 7 mile-per-hour delay in drag rise due to blade twist would have been accurately predicted.

The results shown in figure 6 also indicate that, once stalling was developed on both rotors, the twisted blades required approximately 15 horsepower less to operate at the same speed than did the untwisted blades, the decrease in additional profile-drag power due to blade stall amounting to approximately 40 percent of the average profile-drag power absorbed by the rotors in the unstalled conditions.

It is worthy of mention that the flight conditions corresponding to the highest calculated tip angle of attack obtained with the untwisted blades did not correspond to the limit of operation of the helicopter as set by excessive vibration and control difficulties. The helicopter was actually flown at a tip angle of attack that was 1° higher than the angle

of attack shown by the highest data point in figure 5(a). The 1° increment in tip angle corresponds to an increase in airspeed of 6 miles per hour. At the limiting condition, however, the severe shaking of the helicopter and the control difficulties encountered did not permit the measurement of accurate performance data. Thus, the conclusion drawn from the analysis of the twisted-blade data (reference 8) - namely, that the limiting condition of operation corresponds to a calculated tip angle of attack that exceeds the stalling angle by about 4° - is confirmed by the untwisted blade data. It follows that the increase in the limiting forward speed brought about by the use of -8° of twist is equal to the 7 mile-per-hour delay in drag rise shown in figure 6 for the twisted blades.

Vertical autorotative descent.- Rotor drag coefficients and related data obtained in the power-off vertical-descent condition with the untwisted test rotor are listed in table III. The data are compared in figure 7 with values of drag coefficient previously obtained with the twisted blades and with calculations made by a semiempirical theory (reference 7) representing blades having solidities of 0.10 and 0.04. The theory makes no allowance for blade twist. Rotor drag coefficients, which are a measure of the lifting ability of the rotor in vertical descent, are plotted in this figure against the ratio of thrust coefficient to solidity, which represents the rotor mean lift coefficient. The agreement between the data for the untwisted and the twisted blades shown in figure 7 is significant in that it indicates that negative blade twist does not affect by more than a few percent the lifting effectiveness of a rotor in vertical autorotative descent. The average vertical rate of descent of the test helicopter, weighing 2625 pounds at standard sea-level conditions is calculated from the data of figure 7 to be approximately 2400 feet per minute and would be the same for either test rotor.

A comparison between the theoretical calculations and the experimental twisted-blade data reveals that, on the average, the semiempirical theory overestimates the rotor drag coefficient by approximately 12 percent or underestimates the measured rate of descent by approximately 6 percent. The results correspond to the results given in reference 3 for the twisted-blade data; thus the conclusion drawn in this reference concerning the degree of accuracy of the existing theory which covers the vertical-autorotative-descent condition is substantiated. The comparison between the semiempirical theory and the data suggests that, if a more precise agreement is desired, the empirical part of the procedure should be investigated. Such an investigation would involve repeating the basic measurements relating the total flow through the disk in vertical descent to the rate of descent with rotors having different plan-form shapes and surface conditions.

Forward-flight climbs and autorotative glides.- Climb data, which were incidentally obtained in conjunction with the main set of test runs, are presented in table I and derived parameters, in table II. Inasmuch as most of the measurements were obtained with various degrees of blade

stall, they were analyzed directly in terms of the ratio of experimental to theoretical rotor profile-drag-lift ratios and calculated tip angles of attack. These parameters are plotted in figure 5(a), together with the points obtained in level flight. The results indicate that several effects of blade stalling on rotor performance are similar in level flight and in climb. The theory increasingly underestimates the power expended in profile drag as the tip angle of attack exceeds the blade-section stalling angle of attacks. These conclusions are the same as those drawn for the climb results obtained with the twisted blades in reference 3.

A closer examination of the climb data in figure 5(a), as well as those given in figure 5(b) for the twisted blades, suggests however, a somewhat higher and earlier occurrence of profile-drag stalling losses than obtained in level flight. This difference in stalling characteristics implies that rotor theory, and particularly the tip-angle criterion, is not as accurate for large rates of climb as for level flight. A difference in accuracy for the two conditions might be expected inasmuch as the theory was developed specifically for level flight and moderate rates of climb, wherein the usual assumptions regarding the trigonometric functions of small angles are valid.

Two long autorotative glides were also obtained with the untwisted blades. These data are listed in tables I and II, and are shown in figure 8 in terms of rotor drag-lift ratios and tip-speed ratios. Theoretical performance curves, representing the extreme values of measured thrust coefficient, are also shown in the figure, together with the measured autorotative performance of the twisted rotor as given in reference 3. Although it is not possible to draw any general conclusions from a few data points, some significance can be attached to the fact that within the general scatter of the data, the autorotative performance of both rotors are the same, so that negative twist might be expected to have little effect on this condition. The experimental data are also noted to be in good agreement with the theoretical curves, the theory predicting no significant difference between the two rotors.

CONCLUSIONS

A comparison of flight-performance measurements made on an untwisted, plywood-covered rotor with measurements on a similar rotor having 8° of linear washout, indicates the following conclusions:

1. Negative blade twist appears to be an effective means for increasing the maximum forward speed of the helicopter as limited by blade stall and for reducing the performance losses due to stall at a given thrust coefficient and tip-speed ratio.
2. An increase of approximately 7 miles per hour or about 10 percent in the limiting speed of the test helicopter appears possible with the use of -8° of blade twist. In terms of power savings, the 7 miles per

hour increase in limiting speed represents, at a specific airspeed, a reduction of approximately 15 horsepower from the profile-drag power absorbed by the untwisted blades, once stalling had developed on both rotors. This reduction in power amounts to approximately 40 percent of the average profile-drag power absorbed by the rotors in the unstalled condition.

3. Negative blade twist has little effect on the rate of descent of the helicopter in the vertical-autorotative-flight condition.

4. On the basis of limited data obtained in forward-flight autorotative glides, negative twist appeared to have little influence on the rotor drag-lift ratios in that condition.

Langley Aeronautical Laboratory

National Advisory Committee for Aeronautics

Langley Field, Va., April 22, 1948

REFERENCES

1. Gustafson, F. B., and Gessow, Alfred: Effect of Rotor-Tip Speed on Helicopter Hovering Performance and Maximum Forward Speed. NACA ARR No. L6A16, 1946.
2. Gustafson, F. B., and Myers, G. C., Jr.: Stalling of Helicopter Blades. NACA TN No. 1083, 1946.
3. Gustafson, F. B., and Gessow, Alfred: Analysis of Flight-Performance Measurements on a Twisted, Plywood-Covered Helicopter Rotor in Various Flight Conditions. NACA TN No. 1595, 1947.
4. Gustafson, F. B.: Flight Tests of the Sikorsky HNS-1 (Army YR-4B) Helicopter. I - Experimental Data on Level Flight Performance with Original Rotor Blades. NACA MR No. L5C10, 1945.
5. Gessow, Alfred and Myers, Garry C., Jr.: Flight Tests of a Helicopter in Autorotation, Including a Comparison with Theory. NACA TN No. 1267, 1947.
6. Bailey, F. J., Jr., and Gustafson, F. B.: Charts for Estimation of the Characteristics of a Helicopter Rotor in Forward Flight. I - Profile Drag-Lift Ratio for Untwisted Rectangular Blades. NACA ACR No. L4H07, 1944.
7. Wheatley, John B.: An Aerodynamic Analysis of the Autogiro Rotor with a Comparison between Calculated and Experimental Results. NACA Rep. No. 487, 1934.
8. Gustafson, F. B., and Gessow, Alfred: Effect of Blade Stalling on the Efficiency of a Helicopter Rotor as Measured in Flight. NACA TN No. 1250, 1947.

TABLE I

SUMMARY OF DATA OBTAINED IN THE LEVEL-FLIGHT, CLIMB, AND AUTOCROTIC-CLIMB CONDITIONS WITH UNFLEXED BLADES

Test run	Cali- brated airspeed V_a (mph)	Density ratio ρ/ρ_0 (av.)	True airspeed V (mph)	Gross weight W (lb)	Rotor speed (rpm)	Engine speed (rpm)	Rate of climb V_v (ft/min)	Atmos- pheric pressure (in. Hg) (av.)	Free- air temper- ature (°F)	Intake air temper- ature (°F)	Manifold pressure (in. Hg)	Brake horsepower (Engine- power charts)	Main rotor power (hp)	Pitch angle (deg)		Shaft inclina- tion (nose down) (deg)
														Main rotor	Tail rotor	
1	43.6	0.928	45.3	2657	223	2080	0	28.10	66	78	-----	-----	90	10.6	1.5	-2.0
2	43.8	.885	46.6	2645	225	2100	0	26.60	62	74	-----	-----	92	10.6	1.2	-2.2
3	43.0	.884	45.7	2639	240	2240	0	26.47	60	72	-----	-----	98	11.5	2.2	-2.0
4	42.0	.876	44.9	2630	217	2024	0	-----	63	75	-----	-----	107	12.4	2.2	-2.0
5	61.0	.865	65.5	2618	241	2252	0	26.02	60	72	-----	-----	124	11.8	1.3	-5.7
6	60.0	.859	64.7	2633	245	2292	0	24.51	36	49	-----	-----	116	10.1	1.4	-5.7
7	60.0	.860	64.7	2621	235	2198	0	24.97	36	48	-----	-----	133	11.5	1.6	-5.7
8	68.0	.853	73.6	2609	246	2294	0	24.40	36	48	-----	-----	135	11.2	1.5	-7.6
9	42.8	.970	43.4	2649	245	2292	0	28.51	50	60	-----	-----	94	8.5	1.4	-1.3
10	49.5	.928	51.4	2643	234	2188	0	27.26	50	59	-----	-----	90	9.7	1.2	-2.4
11	60.0	.927	62.3	2637	240	2242	0	27.20	49	58	-----	-----	104	10.2	1.4	-4.1
12	68.8	.930	71.4	2622	240	2242	0	27.26	49	58	-----	-----	134	11.2	1.1	-5.9
13	71.5	.929	74.2	2610	239	2232	0	27.22	49	58	-----	-----	144	12.2	1.6	-6.9
14	65.0	.927	67.5	2601	241	2252	0	27.16	48	57	-----	-----	119	10.8	1.0	-5.3
15	48.8	.971	49.5	2583	244	2282	0	28.49	49	59	-----	-----	93	8.6	1.1	-2.9
16	45.0	.903	47.4	2671	241	2250	404	27.75	73	84	26.66	171	140	10.9	3.1	-1.8
17	46.5	.900	49.0	2656	232	2164	388	27.75	75	86	26.25	163	138	12.0	2.7	-2.4
18	45.5	.880	48.5	2635	227	2118	256	26.93	72	83	26.25	161	131	12.5	3.0	-2.5
19	45.0	.910	47.2	2668	241	2250	456	27.54	65	75	24.50	158	136	10.7	2.5	-2.3
20	40.0	.890	42.4	2677	229	2140	406	26.87	64	70	-----	-----	137	11.9	3.1	-1.3
21	45.5	.900	48.0	2671	230	2150	398	26.92	60	68	25.77	161	138	10.7	2.7	-2.4
22	40.8	.905	43.0	2693	241	2250	531	27.25	63	71	25.03	162	145	10.9	3.2	-2.4
23	41.5	.910	43.5	2698	237	2210	524	27.44	64	72	25.23	163	142	-----	-----	-1.5
24	39.0	.924	30.2	2669	228	2130	475	28.14	68	78	-----	-----	141	11.4	3.2	-5.4
25	49.5	.930	51.4	2665	218	2040	-1155	28.15	65	-----	-----	-----	-5.1	5.9	-1.8	-2.6
26	47.0	.942	48.4	2663	232	2170	-1105	28.22	72	-----	-----	-----	-6.0	9.9	-1.4	-2.6

NACA

TABLE II

WING DRAG-LIFT RATIOES AND RELATED PARAMETERS IN THE LEVEL-GLIDE,
 (ZERO, AND AUTOCENTRIC-DRAG CORRECTIONS) WITH UNIFORM REAR

Test run	V_o (mph)	V (mph)	V_r (ft/min)	γ (deg)	θ (deg)	α (deg)	β	$C_{L_{max}}$	ΔC_L (deg)	ΔC_D (deg)	C_L	C_D	$\frac{C_L}{C_D}$	C_D	$\frac{C_L}{C_D}$	$\left(\frac{C_L}{C_D}\right)_P$	$\left(\frac{C_L}{C_D}\right)_D$	$\left(\frac{C_L}{C_D}\right)_O$	$\left(\frac{C_L}{C_D}\right)_E$	$\Delta(L/D)$ (deg)	$\frac{(C_L/D)_{max}}{(C_L/D)_{min}}$
1	43.6	45.3	0	0	10.6	6	0.149	0.463	-6.9	-8.9	0.497	11.84	0.0075	0.278	0.040	0.0085	0	0.296	13.8	1.100	
2	43.8	46.6	0	0	10.6	6	.152	.477	-6.8	-9.0	.487	11.60	.0076	.278	.040	.0083	0	.296	14.3	1.173	
3	45.0	45.7	0	0	11.5	5	.140	.494	-7.1	-9.1	.502	11.95	.0049	.307	.039	.0082	0	.261	12.9	1.201	
4	42.0	44.9	0	0	12.4	6	.152	.515	-7.4	-9.4	.526	12.72	.0060	.338	.048	.0083	0	.297	15.8	1.600	
5	61.0	65.5	0	0	11.8	9	.197	.644	-3.5	-9.2	.296	6.10	.0070	.266	.078	.0091	0	.189	15.1	1.460	
6	60.0	64.7	0	0	10.1	9	.192	.623	-3.6	-9.3	.298	6.28	.0049	.250	.076	.0090	0	.172	14.5	1.25	
7	60.0	64.7	0	0	11.5	9	.200	.622	-3.6	-9.3	.297	6.26	.0073	.268	.077	.0092	0	.203	16.1	1.72	
8	68.0	73.6	0	0	11.2	11	.217	.795	-2.8	-10.3	.200	4.99	.0049	.297	.099	.0090	0	.194	15.6	1.35	
9	42.8	43.4	0	0	8.5	5	.130	.501	-7.2	-8.5	.505	12.12	.0083	.303	.039	.0081	0	.262	10.6	1.10	
10	49.5	51.4	0	0	9.7	6	.160	.573	-5.3	-7.7	.577	9.07	.0049	.247	.051	.0084	0	.194	13.0	1.00	
11	60.0	62.3	0	0	10.8	8	.169	.623	-3.6	-7.7	.297	6.26	.0047	.234	.075	.0085	0	.196	13.8	1.06	
12	68.8	71.4	0	0	11.2	11	.216	.791	-2.7	-10.6	.195	4.23	.0047	.262	.100	.0096	0	.193	15.6	1.38	
13	71.5	74.2	0	0	12.2	12	.224	.776	-2.5	-9.4	.181	4.30	.0047	.272	.109	.0099	0	.199	16.0	1.47	
14	65.0	67.5	0	0	10.8	10	.203	.613	-3.0	-8.4	.217	5.33	.0046	.249	.090	.0092	0	.196	14.4	1.22	
15	48.8	49.5	0	0	8.6	6	.149	.576	-5.4	-8.3	.580	9.12	.0042	.271	.051	.0082	0	.218	11.1	1.13	
16	49.0	47.4	454	6.2	10.9	5	.144	.493	-6.5	-14.5	.441	11.0	.0048	.410	.045	.0088	.110	.294	12.8	1.24	
17	46.5	49.0	398	5.2	12.0	6	.155	.484	-6.1	-13.6	.422	10.2	.0051	.394	.047	.0083	.090	.295	14.7	1.42	
18	45.5	48.5	256	3.4	12.5	6	.156	.439	-6.3	-12.2	.446	10.7	.0075	.380	.044	.0083	.060	.273	14.9	1.50	
19	45.0	47.2	456	6.3	10.7	5	.143	.491	-6.5	-15.0	.429	11.0	.0047	.358	.046	.0082	.110	.240	12.7	1.10	
20	40.0	42.4	406	6.2	11.9	5	.136	.574	-8.2	-15.7	.522	13.9	.0074	.449	.036	.0081	.104	.301	14.3	1.28	
21	45.5	48.0	398	5.4	10.7	6	.153	.444	-6.4	-14.2	.422	10.7	.0075	.399	.045	.0083	.094	.296	14.5	1.40	
22	40.8	43.0	531	8.1	10.9	5	.131	.543	-7.8	-17.3	.573	13.0	.0047	.472	.040	.0081	.142	.288	12.3	1.17	
23	41.5	43.5	524	7.8	---	5	.135	.524	-7.9	-16.8	.533	12.6	.0048	.441	.041	.0081	.137	.281	12.9	1.19	
24	49.0	50.2	473	10.3	11.4	10	.094	1.077	-15.4	-20.3	1.029	-7.7	.0039	.620	.023	.0018	.122	.423	10.8	1.02	
25	49.5	51.4	-1195	-14.8	5.9	7	.172	.563	-5.2	-7.0	.524	8.6	.0075	-0.043	.049	.0085	-1.264	.198	---	---	
26	47.0	48.4	-1195	-15.0	9.9	7	.153	.403	-5.8	-6.6	.404	9.6	.0048	-0.080	.043	.0083	-2.269	.205	---	---	

NACA

TABLE III
 VERTICAL-AUTOROTATIVE-DESCENT DATA OBTAINED
 WITH THE UNTWISTED BLADES

Run	W (lb)	ρ/ρ_0	Free-air temperature (°F)	Atmospheric pressure (in. Hg) (av.)	V_v (fpm)	Rotor speed (rpm)	C_T	Z C_T/σ	C_D
1	2617	0.937	73	28.74	-2580	238	0.0046	0.110	1.12
2	2665	.914	65	27.62	-2540	236	.0049	.115	1.21
3	2662	.955	63	28.74	-2380	241	.0045	.107	1.32
4	2652	.942	52	27.76	-2430	215	.0057	.135	1.27
5	2634	.944	52	27.83	-2390	220	.0054	.128	1.30
6	2655	.933	53	27.46	-2500	224	.0054	.128	1.21
7	2637	.885	52	26.04	-2540	229	.0053	.126	1.23
8	2637	.925	51	27.22	-2393	229	.0051	.121	1.32





Figure 1.- Test helicopter equipped with an untwisted, plywood-covered set of main-rotor blades.

Main rotor:	
Radius, ft	19
Blade area (3 blades), sq ft	65.4
Disk area, sq ft	1134.1
Solidity	0.060
Ratio of rotational speed to engine speed	0.107
Tail rotor:	
Radius, ft	3.96
Blade area (3 blades), sq ft	4.92
Disk area, sq ft	49.2
Ratio of rotational speed to engine speed	0.567
Center line of main rotor to center line of tail rotor, ft	25.19
Parasite-drag area, sq ft	22.92
Rated horsepower	180

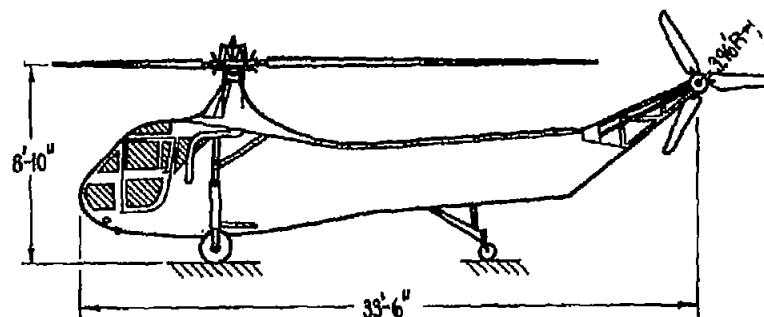
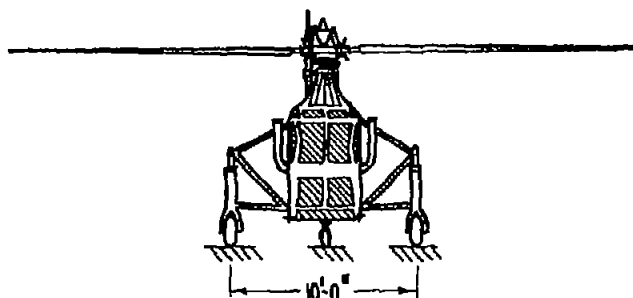
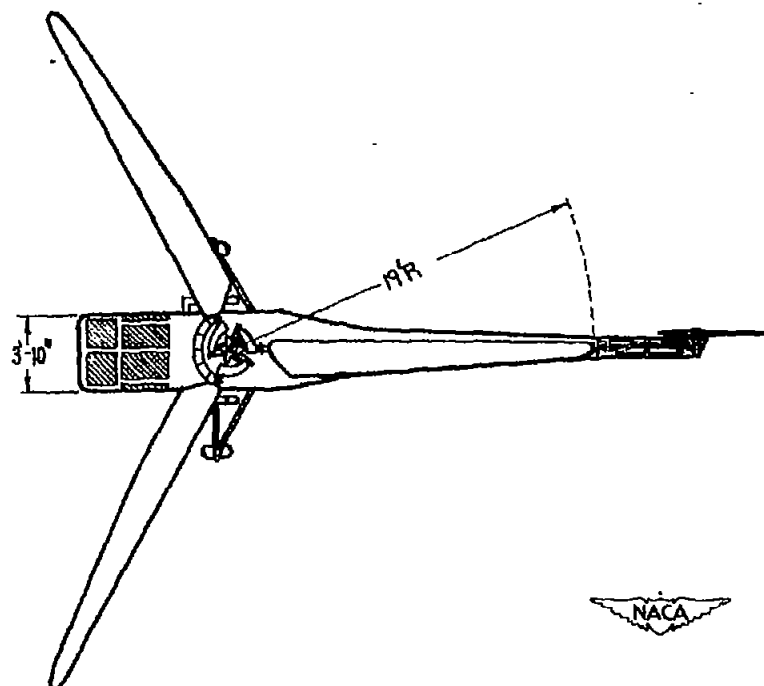


Figure 2.- Dimensions and pertinent characteristics of test helicopter.

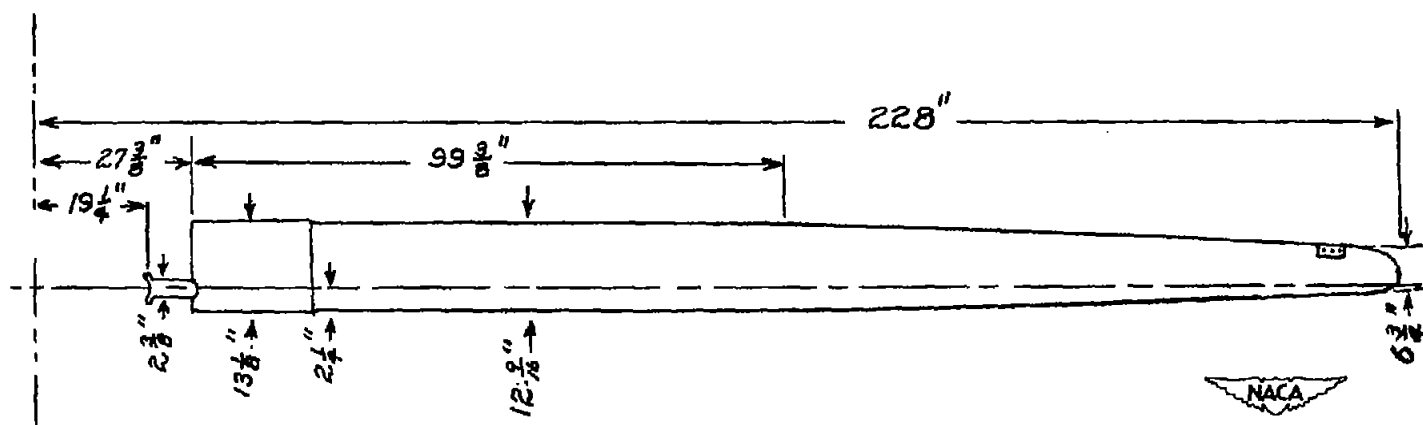
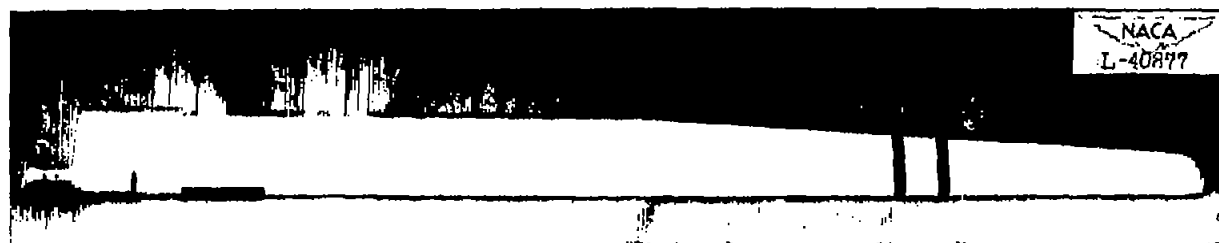


Figure 3.- General view and plan-form dimensions of test rotor blade.

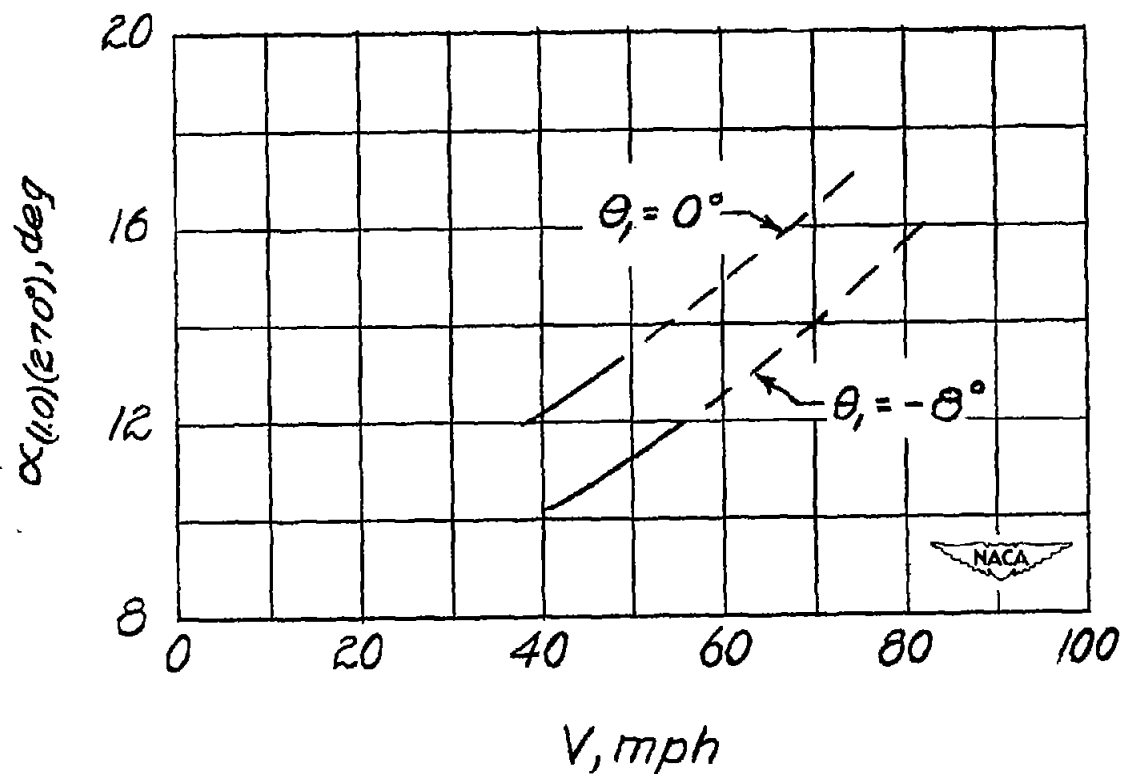
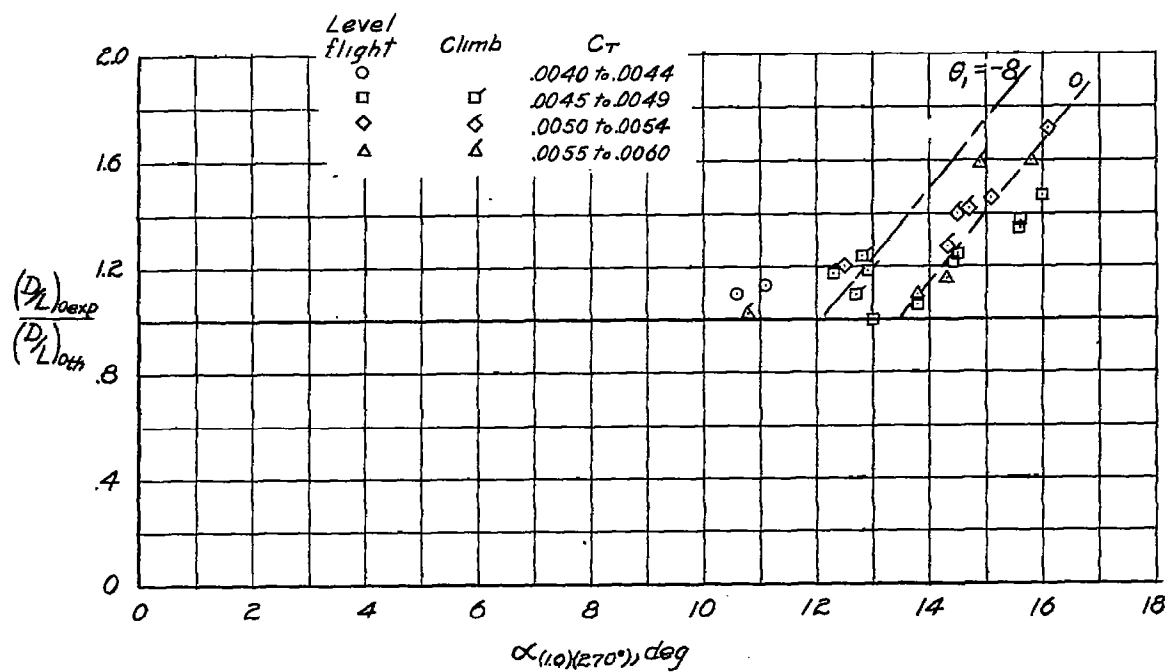
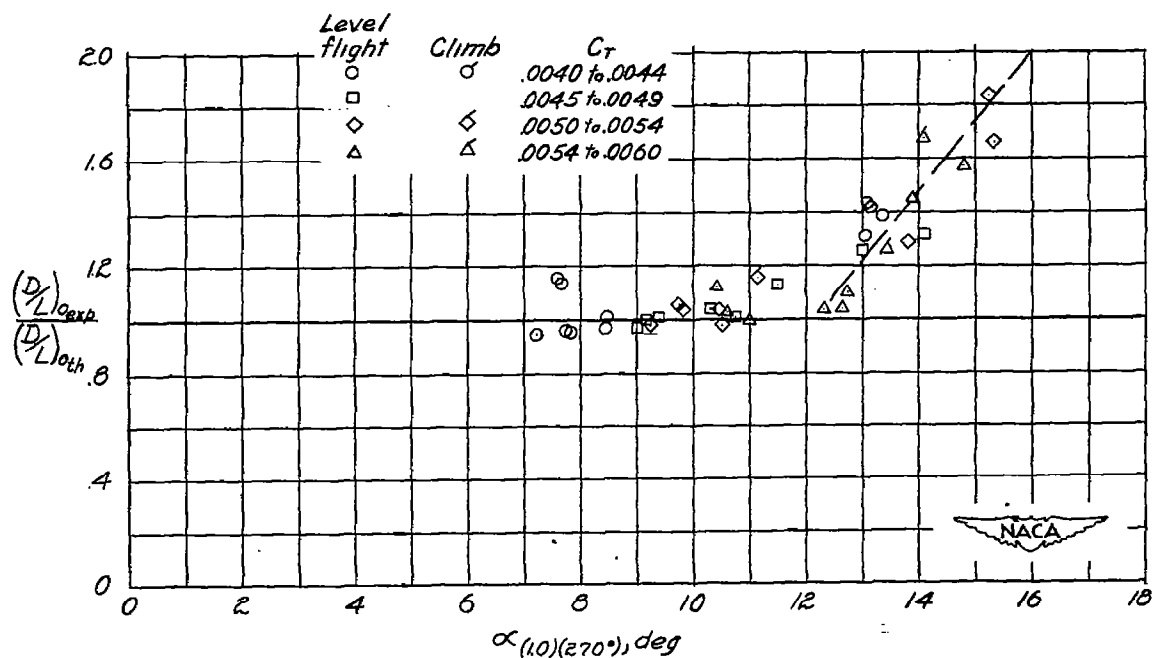


Figure 4.- Theoretical effect of blade twist on the calculated blade-tip angles of attack and limiting forward speed of test helicopter. $W = 2625$ pounds; $\Omega R = 465$ feet per second; $C_T = 0.0050$.



(a) Untwisted-blade data.



(b) Twisted-blade data (from reference 3).

Figure 5.- Stall analysis of data obtained with test rotors in level flight and in climb.

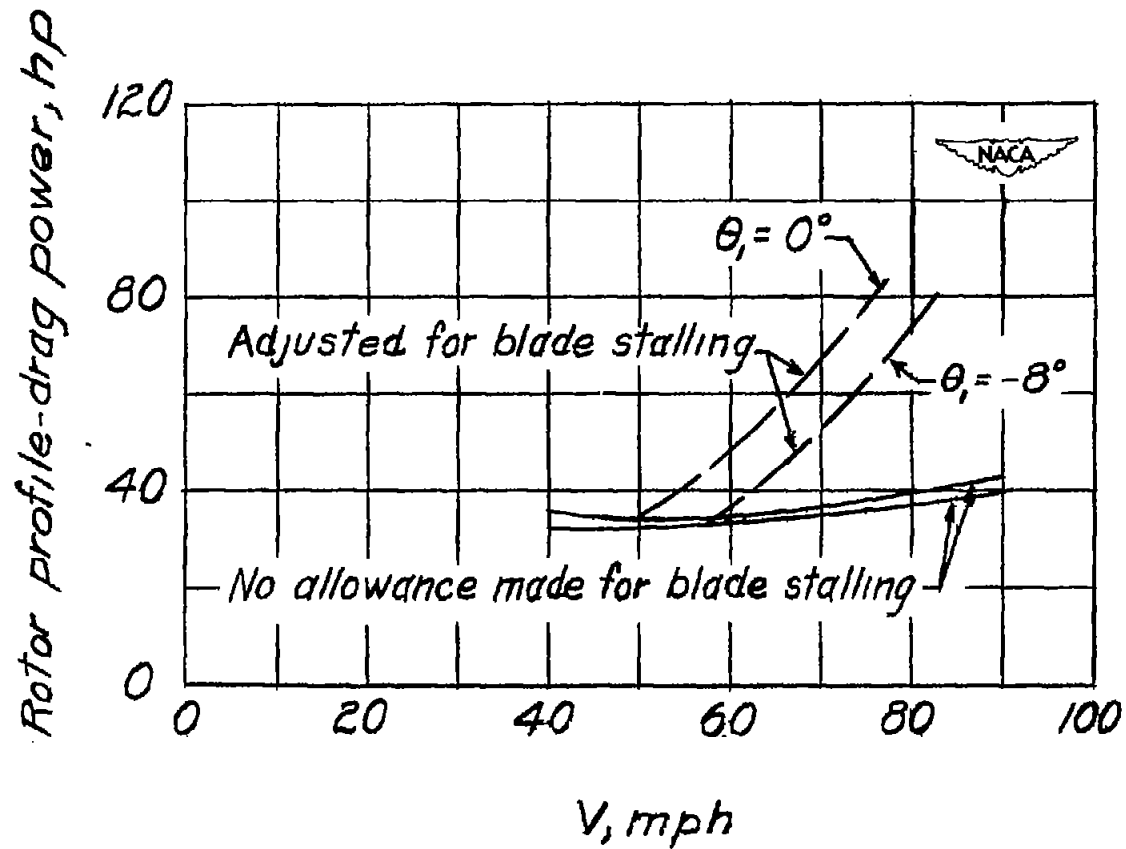


Figure 6.- Effect of blade twist on rotor profile-drag power for test helicopter.
 $W = 2625$ pounds; $\Omega R = 465$ feet per second; $C_T = 0.0050$.

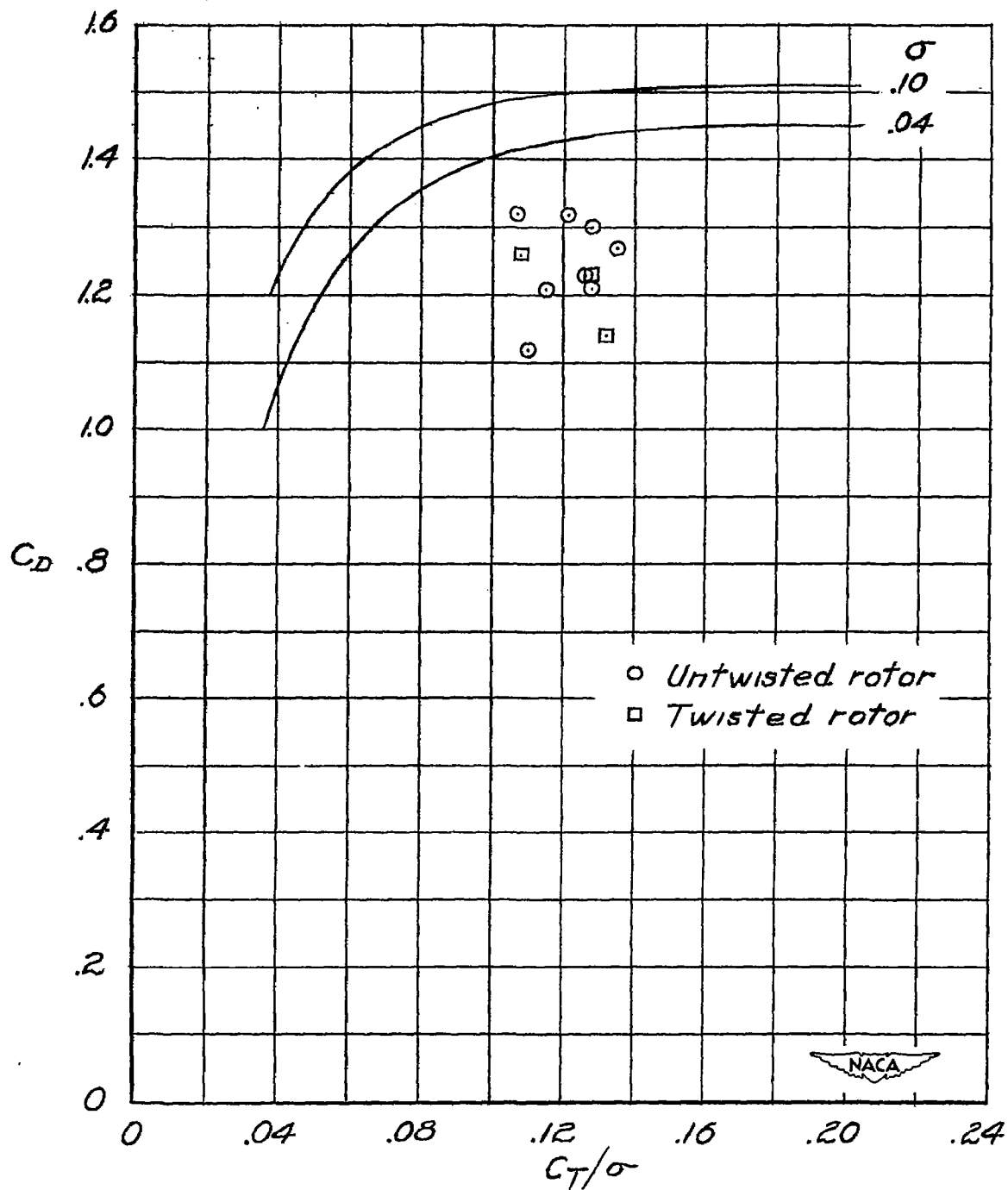


Figure 7.- Comparison of the vertical autorotative performance of untwisted blades with that of twisted blades and with results obtained by semiempirical theory.

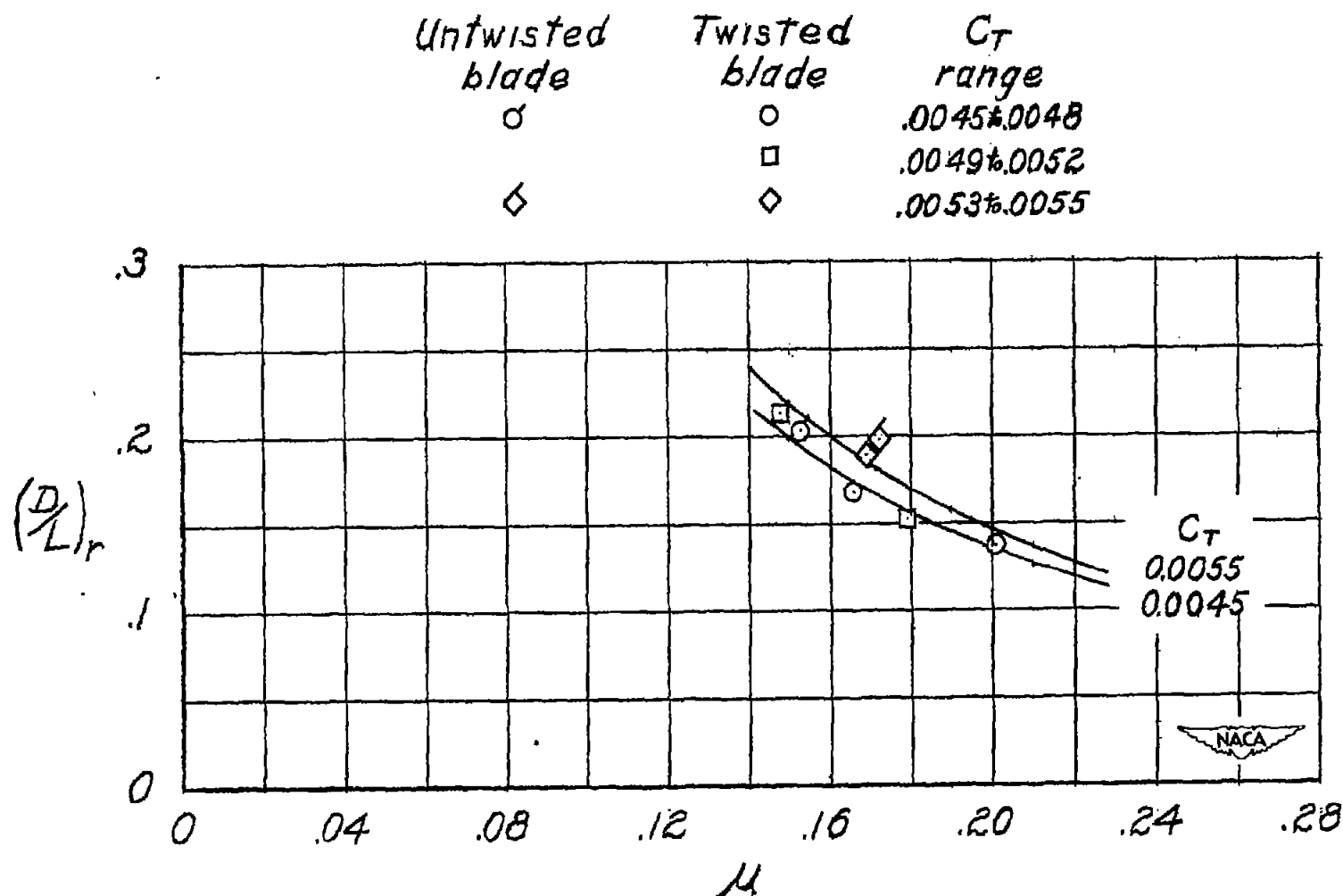


Figure 8.- Comparison of the autorotative glide performance of the untwisted blades with the performance of the twisted blades and with theoretical results.